

01.5;09.5

Influence of the structure of the wavefront of laser radiation on synchronous self-oscillations in fiber lasers with micro-optomechanical resonators

© F.A. Egorov

Fryazino Branch, Kotel'nikov Institute of Radio Engineering and Electronics, Russian Academy of Sciences, Fryazino, Moscow oblast, Russia
E-mail: egorov-fedor@mail.ru

Received October 22, 2021

Revised January 31, 2022

Accepted February 1, 2022

It is shown, that increasing the stability of synchronous self-oscillations in fiber lasers with nonlinear mirrors, based on micro-optomechanical resonators (micro-oscillators), can be achieved due to the transformation of the wavefront of laser radiation, interacting with micro-oscillators. These transformations are based on the unique properties of mode interference in composite singlemode-multimode-singlemode fiber structures.

Keywords: synchronous self-oscillations, fiber lasers, microcantilever, resonance.

DOI: 10.21883/TPL.2022.04.53168.19060

Micro-oscillators (micro-optomechanical resonators, MOMR) provide an opportunity to implement novel and promising laser operation regimes with unique characteristics of radiation [1–4]. The laser excitation of elastic oscillations in micro-oscillators in fiber lasers (FL) with micro-oscillators allows one to implement synchronous self-oscillation (SSO) regimes with the radiation parameters modulated at frequencies close to the eigenfrequencies (f) of elastic MOMR oscillation modes: $F = (1 + \chi)f$, $\chi \ll 1$ [5]. This may be used to stabilize the pulse frequency in fiber pulsed laser sources (similar to „quartz“ stabilization in radio engineering) and may serve as a basis for the design of a new class of resonance fiber-optic sensors [6,7].

The dynamics of FL–MOMR laser systems depends to a considerable extent on the conditions of interaction between micro-oscillators and laser radiation, which govern, amongst other things, the efficiency of excitation of elastic oscillations and the nature and depth of modulation of a light wave. Note that the influence of such an important factor as the wave-field structure on the interaction of radiation with elastic MOMR oscillations and on self-oscillations in FL–MOMR remains understudied. The structure of the wave front of laser (coherent) radiation in fiber-optic systems may be controlled efficiently via multimode interference in composite singlemode–multimode (SM) and singlemode–multimode–singlemode (SMS) fibers [8,9]. This makes the studies into FL–SM(S)–MOMR laser systems highly relevant.

Experiments were performed using an erbium-ytterbium fiber laser (EYDFL) with diode pumping and the micro-oscillator acting as a mirror (M) of the laser cavity (Fig. 1). The double-clad active fiber (AF) was pumped by continuous radiation of the pumping diode ($\lambda_p \approx 0.98 \mu\text{m}$), which was directed to the inner AF cladding ($d_{cl} \approx 105 \mu\text{m}$)

by the multimode fiber-optic splitter. The same splitter was used to detect the EYDFL radiation ($\lambda_s \approx 1540 \text{ nm}$). The single-mode AF core with diameter $d_{co} \approx 9 \mu\text{m}$ was doped with erbium and ytterbium with concentrations ($N_{Er}; N_{Yb}$) $\approx (5 \cdot 10^{24}; 1.5 \cdot 10^{26} \text{ m}^{-3})$, the AF length and the length of the fiber-optic EYDFL cavity were ($L_{AF}; L$) $\approx (0.9; 1 \text{ m})$, the reflection coefficients of the semi-transparent dichroic mirror (M_0) were $r_0(\lambda_s) \approx 95\%$, $r_0(\lambda_p) < 6\%$, and the envelope width of single-mode multifrequency laser radiation was $\Delta\lambda_s \lesssim 1 \text{ nm}$. The mean power of laser radiation incident on the micro-oscillator could be adjusted within $\bar{P}_s = 0–8 \text{ mW}$ by varying the pumping power (P_p).

Silicon micro-oscillators with oscillating elements in the form of microcantilevers (MC), which differed in the parameters of elastic oscillation modes, their optical properties, and size, were used in experiments: MC₁, MC₂. The surface of MC₁ interacting with laser radiation was coated with a thin nickel film ($\sim 120 \text{ nm}$) with reflection and absorption coefficients $R_1(\lambda_s) \approx 70\%$ and $A_1(\lambda_s) \approx 30\%$, and the working surface of MC₂ was coated with a multilayer interference ZrO₂ + SiO₂ film with high reflection $R_2(\lambda_s) \approx 98\%$, $A_2(\lambda_s) < 0.1\%$. The difference in optical properties of MC_{1,2} translates into significantly different mechanisms of laser excitation of bending oscillations $U(z, t)$ [10] in them: photothermal excitation due to radiation absorption in the Ni film is predominant in MC₁, while excitation due to light pressure prevails in MC₂. The SM (MMF end face) position relative to MC_{1,2} was set using a three-coordinate micropositioner.

The SM diagram is shown in Fig. 1. We designed an SM with a „transition“ SMF to be used as a substitute for a simplified SM produced by connecting an AF directly to an MMF. This new design helps enhance the SM properties by varying the transition SMF parameters and suppress the

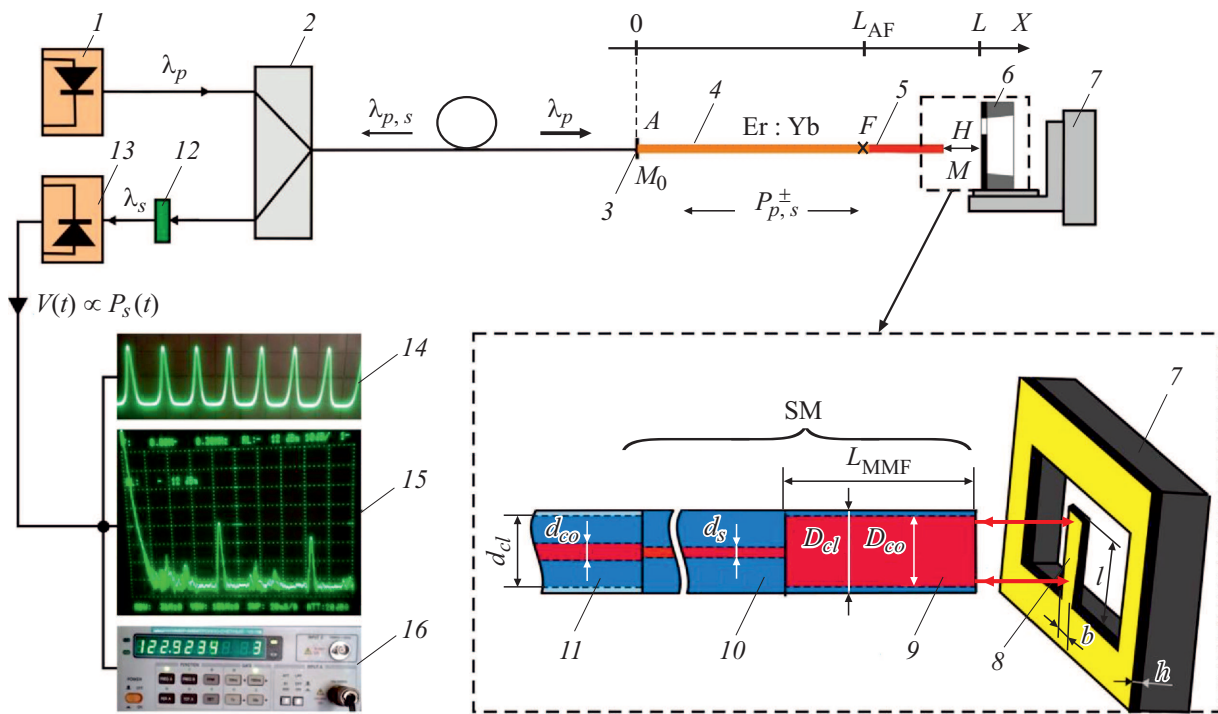


Figure 1. Diagram of the EYDFL–SM–MOMR laser system. 1 — semiconductor pumping laser ($\lambda_p \approx 980$ nm), 2 — fiber-optic splitter (multimode), 3 — dichroic mirror (M_0), 4 — erbium-ytterbium active double-clad fiber, 5 — SM, 6 — MOMR case, 7 — micropositioner ($x-y-z$), 8 — micromirror (M)–silicon microcantilever (MC_1 : $520 \times 75 \times 24 \mu\text{m}$, MC_2 : $660 \times 73 \times 6 \mu\text{m}$), 9 — multimode step-index fiber (MMF), 10 — single-mode fiber (SMF), 11 — AF, 12 — optical filter, 13 — photoreceiver (output signal $V(t) \propto P_s(t)$), 14 — oscilloscope (Tektronix 2465), 15 — radio-frequency spectrum analyzer (Anritsu MS 710C), 16 — frequency meter (Ch3-163). The pulse shape and the Fourier spectrum of laser radiation intensity in EYDFL–SM₂–MC₁ with SSO excitation at the eigenfrequency of the second mode of transverse MC₁ oscillations are demonstrated on the screens of the oscilloscope and the spectrum analyzer. Fibers AF, SM, and MMF are connected by fusion splicing.

residual pumping radiation that penetrates from an AF to an MMF and perturbs the MOMR oscillations. The fraction of radiation power reflected back from the micro-oscillator to the AF was $R_{eff}(t) = R_{1,2}T_s K(t) = \bar{R}_{eff} + r(t)$, where $K(t)$ is the effective coefficient of SM–MOMR optical coupling, which depends on $MC_{1,2}$ oscillations; T_s is the SMS transfer function with a doubled MMF length; and \bar{R}_{eff} , $r(t)$ are the constant and variable components. SM fibers with different types of quartz SMF and MMF were fabricated. The majority of experiments were performed using an SM based on a step-index MMF with size $D_{co}/D_{cl} = 105/125 \mu\text{m}$ and numerical aperture $NA_M = (n_{co}^2 - n_{cl}^2)^{1/2} \approx 0.22$ and SMF (G657A2): $NA_S \approx 0.16$, $d_s \approx 6 \mu\text{m}$. The corresponding typical values of \bar{R}_{eff} are 0.2–0.5.

At $NA_{S,M} \ll 1$, the SM properties are governed primarily by the MMF section parameters [8]. Specifically, the key SM parameter — spatial period (L_0) of „images“ of a coherent radiation source emerging in an MMF as a result of multimode interference — is expressed as $L_0 = 4n_{co}D_{co}^2/\lambda_s$, and the near-field structure in the output MMF section depends on relation $k = L_{MMF}/L_0$. Since $n_{co}(\lambda_s) \approx 1.456$, $L_0 \approx 41.62$ mm for the considered SM fibers. We limit ourselves to the study of three SM types SM_{1–3} with

$k_{1–3} = 1, 1/2, 0.584$. The radial intensity distribution (I_s) of laser radiation in the output MMF section in the case of $k_2 = 1/2$, which is of special interest, is shown in Figs. 2, a, b. This distribution was determined by measuring the optical power entering the receiving SMF (G657A2) through a small gap ($\lesssim 5 \mu\text{m}$) from different regions of the MMF end face. At $k_1 = 1$, radiation is localized almost completely at the center of the output MMF section in the form of a bright spot with diameter $\sim d_s$. This spot is essentially an „image“ of the SMF mode spot. At $L_{MMF} = L_0/2$, the radiation wave front has the form of a thin ring with width $\sim d_s$ positioned along the perimeter of the MMF core. The fraction of power in the weak central spot is $\lesssim 5\%$ of the total MMF power (P_s). At $k_3 \approx 0.584$, the radiating region of the MMF end face has the form of a concentric system with a bright spot at the center and a thin ring along the perimeter of the MMF core. The fractions of power in the spot and in the ring are roughly equal ($\sim P_s/2$). Significantly different conditions of interaction between laser radiation and the micro-oscillator are established in the mentioned cases.

It was found that SSOs with frequencies $F \approx f$ exist in the studied EYDFL–SM_{1–3}–MC_{1,2} laser systems in $f_{rel} \approx f$ ($f_{rel}(P_p)$ is the frequency of relaxation FL os-

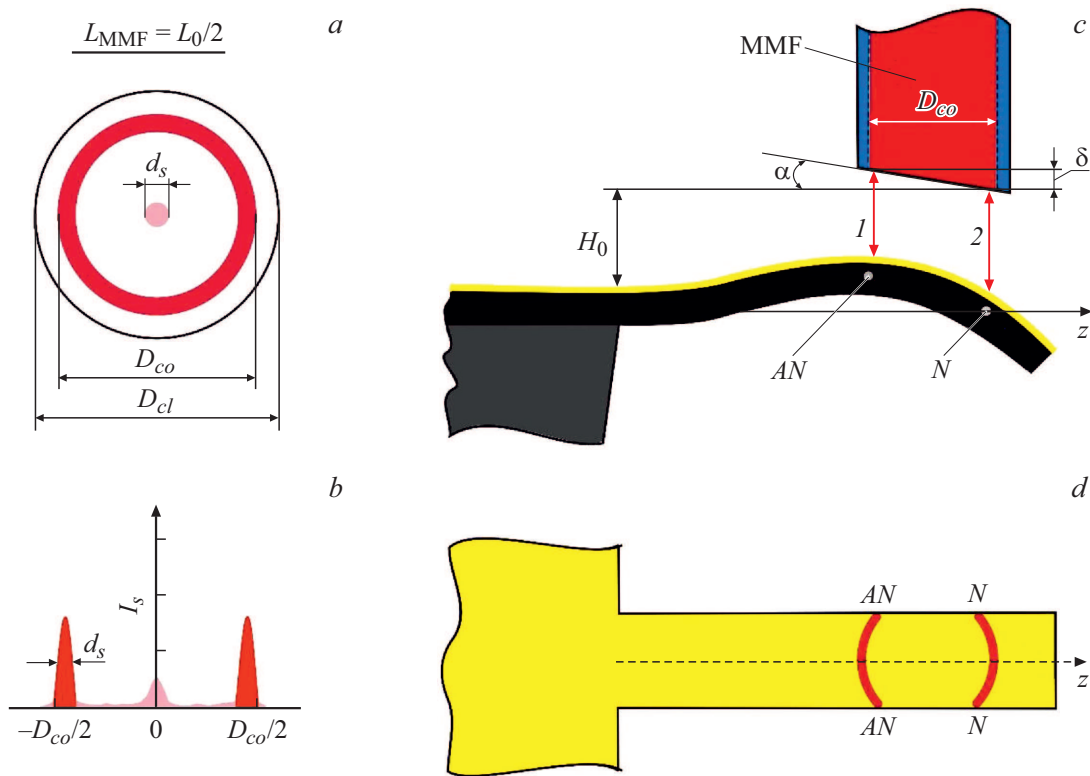


Figure 2. Diagram (a) and profile (b) of the radial intensity distribution of laser radiation in the near-field region of the output MMF section at $k_2 = 1/2$; c — diagram of interaction between the micro-oscillator and laser radiation with an annular wave front under excitation of the second mode of transverse MC_1 oscillations; d — projection of the laser beam onto MC_1 .

cillations) resonance conditions irrespective of the specifics of mechanisms of laser excitation of oscillations, optical MC properties, and the MC design. Resonance and SSO conditions were established (specifically, by adjusting the pumping power) at the first and the second modes of bending oscillations of MC_1 with eigenfrequencies $(f_{1,1}; f_{1,2}) = (22.4; 122.9 \text{ kHz})$ and the first, the second, and the third modes of MC_2 with frequencies $(f_{2,1}; f_{2,2}; f_{2,3}) = (6.9; 38.7; 118.1 \text{ kHz})$, which have mechanical quality factors (in air) $Q_1 = 40\text{--}90$, $Q_2 = 30\text{--}110$. At $k_1 = 1$, owing to the exact equivalence of the characteristics of radiation of the source and its „image“ at the MMF output, the properties of EYDFL– SM_1 – $MC_{1,2}$ and EYDFL– $MC_{1,2}$ laser systems are virtually the same. SSOs arise in them due to the $R_{eff}(t)$ modulation in oscillations of the baseline of the Fabry–Pérot cavity ($H(t) = H_0 + U(t)$) that is formed by the semi-reflective ($\sim 4\%$) MMF (or SMF) end face and the reflective oscillating MC surface (initial baseline $H_0 \lesssim 20 \mu\text{m}$). Owing to the periodicity of $R_{eff}(H)$, baseline variations $\Delta H_0 \geq \lambda_s/2$ change the feedback sign and thus induce SSO quenching.

In view of the complex (distributed) shape of the wave front at the MMF output in $SM_{2,3}$, the signal reflected back to the AF forms as a result of interference of several beams reflected from different regions of the MC surface (Figs. 2, c, d) that undergo different deformations in the process of oscillation. In the context of SSO existence, the

reflection from the MMF end face ($\sim 4\%$) does not play a significant part here (in contrast to designs with SM_1), since both the translational MOMR displacement, which alters the $\Delta H_0 \geq \lambda_s/2$ gap, and the antireflection coating of the MMF end face had almost no effect on SSOs. This is attributable to the fact that the SSO-inducing R_{eff} modulation depends in this case primarily on the phase difference of interfering beams; their common increments of optical lengths due to the MOMR displacement are compensated, while the „background“ reflection from the MMF end face ($\sim 4\%$) has almost no effect on the modulated $r(t)$ component. Thus, the transformation of the wave front with $SM_{2,3}$ in FL–MOMR enhances the SSO stability.

At the same time, the indicated forms of wave fronts in $SM_{2,3}$ allow one to establish such conditions in FL–MOMR that ensure high efficiency both of the laser excitation of MC oscillations and of radiation modulation in the process of its oscillations (key SSO factors). Note that the regions of radiation focusing on the microcantilever corresponding to the maxima of MC oscillation amplitude and the radiation modulation depth are specified by significantly different conditions and normally have different coordinates. These conditions depend, e.g., on the mode and the mechanism of excitation of elastic oscillations [10] and the modulated parameter of a light wave (amplitude, phase, etc.). The considered laser systems provide an opportunity to optimize the interaction between the micro-oscillator and laser

radiation due to the fact that different parts of the wave front may be localized in the regions of efficient oscillation excitation and the maximum modulation depth. As a result, the net effect of both factors is enhanced. This approach is applicable, e.g., when higher MC oscillation modes with antinodes (AN) and stationary nodes (N) are excited; it is then expedient to position different parts of the wave front near a node and at an antinode. This is confirmed, among other things, by the results of examination of SSOs excited in EYDFL–SM₂–MC₁ at frequency $F_2 \approx 122.9$ kHz of the second MC₁ oscillation mode (Figs. 1 and 2, *c, d*), where radiation incident at the AN region excites oscillations efficiently, while the interference of beams $I, 2$ reflected in the AN and N regions provides efficient $R_{eff}(t)$ modulation. The „quadrature“ condition for these beams was implemented through small-angle ($\alpha = \delta/D_{co} \approx 0.12^\circ$) polishing of the MMF end face that provides the initial optimum phase shift between beams $I, 2$: $2\delta(n_{co} - 1) = \lambda_s/8$. As a result, SSOs in this laser system at the frequency of the second MC₁ oscillation mode had short-term frequency (period) stability $|\Delta F_2/F_2|_{ft} \approx 6 \cdot 10^{-6}$ (the averaging time of the frequency meter was 0.1 s), and the „long-term“ instability of the SSO frequency in normal conditions determined in two-month-long continuous observations (without SSO quenching) did not exceed $|\Delta F_2/F_2| \approx 10^{-5}$. In our view, it is appropriate to use SM₃ in FL–MOMR in SSO excitation, e.g., at axially symmetric modes of elastic oscillations of micro-oscillators (specifically, micromembranes).

Thus, the transformation of the structure of the wave front of laser radiation interacting with elastic oscillation modes in fiber lasers with micro-oscillators allows one to enhance the SSO stability and long-term stability. Regardless of the mechanism of laser excitation of elastic oscillations, the opportunities for interaction optimization, which induces the mentioned positive effects, broaden considerably as the harmonics of excited modes grow.

Funding

This study was carried out under the state assignment of the Kotelnikov Institute of Radio Engineering and Electronics of the Russian Academy of Sciences.

Conflict of interest

The author declares that he has no conflict of interest.

References

- [1] W. Yang, S.A. Gerke, K.W. Ng, Y. Rao, C. Chase, C.J. Chan-Hasnain, *Sci. Rep.*, **5**, 13700 (2015). DOI: 10.1038/srep13700
- [2] M. Fabert, A. Desfarges-Berthelot, V. Kermene, *Opt. Express*, **20**, 22895 (2012). DOI: 10.1364/OE.20.022895
- [3] D. Princepe, G.S. Wiederhecker, I. Favero, N.C. Frateschi, *IEEE Photon. J.*, **10**, 4500610 (2018). DOI: 10.1109/JPHOT.2018.2831001
- [4] X. Xiang, M. Jingwen, S. Xiankai, *Phys. Rev. A*, **99**, 053837 (2019). DOI: 10.1103/PhysRevA.99.053837
- [5] F.A. Egorov, V.T. Potapov, *Quantum Electronics*, **50** (8), 734 (2020). DOI: 10.1070/QEL17116.
- [6] F.A. Egorov, V.T. Potapov, *Foton-Ekspress*, №. 7, 4 (2018). <http://fotonexpres.ru/bez-rubriki/vyshel-iz-pechati-foton-ekspress-7>
- [7] E. Buks, I. Martin, *Phys. Rev. E*, **100**, 032202 (2019). DOI: 10.1103/PhysRevE.100.032202
- [8] X. Zhu, A. Schulzgen, H. Li, L. Li, L. Han, J.V. Moloney, N. Peyghambarian, *Opt. Express*, **16**, 632 (2008). DOI: 10.1364/OE.16.016632
- [9] G. Bawa, K. Dandapat, G. Kumar, I. Kumar, S.M. Tripathi, *IEEE Sensors J.*, **19**, 6756 (2019). DOI: 10.1109/JSEN.2019.2913801
- [10] D. Ma, J.L. Garrett, J.N. Munday, *Appl. Phys. Lett.*, **106**, 091107 (2015). DOI: 10.1063/1.4914003